P. vivax parasite material

We obtained *P. vivax* parasite material from individual adults presenting themselves to the Centro de Pesquisa em Medicina Tropical (CEPEM) in Rondônia, Brazil. These studies received ethical clearance from a local executive committee, and all patients consented to donate their blood.

Pulsed-field electrophoresis and Southern analysis

P. vivax chromosomal DNA was isolated from patients as described[10] and size fractionated by pulsed-field gel electrophoresis using a Bio-Rad CHEF-DRII system (pulsed-field conditions: ramped pulse from 90 to 300 s over 24 h at 5.5 V cm^{-1} followed by a ramped pulse from 300 to 700 s over 24 h at 4.0 V cm^{-1} and a final ramped pulse from 700 to 1,200 s over 24 h at 2.5 V cm^{-1}; 1% LE agarose (FMC); running buffer 0.5× TBE at 14 °C. Pulsed-field conditions for telomeric YAC clones have been described[10].

Primers

We used the following degenerate oligonucleotides specific for *vir* subfamilies (5′ to 3′): *vir A*, TATTT(A/G)AATT(A/T)TTGGCTA(A/G)A(C/T)(A/G)A(A/G) and (A/G)(C/T)ATTT(A/T/G)GG(A/G)AATGTTTTAG(C/G)(A/C)ATAT(C/T)AT(A/G); *vir B*, GT(A/T/C)AA(A/T)(A/G)A(A/T)CT(C/T)(C/T)TA(A/G)(A/G)(A/T/G)(A/G)A(A/T)-(A/C)T(C/T)(C/T)A(C/T)AGC(A/C)ATTTA and AGAAGTTGCTGCAATAGTGGT; *vir C*, CT(T/G)TT(A/C/G)AA(C/T)TA(C/T)TGGAT(A/G)TA(C/T) and TAC(C/T)(C/T)TATATAA(A/G)GC(A/G)CCAGA(A/T/G)GT(C/G)AT(A/T)G(A/T); *Pvstp1*, CTAGTAACATCATAGAACAC and TTGTTTCCATTCACTCTTTAAC.

RT–PCR

We prepared and analysed *P. vivax*, *P. falciparum* and human RNA by RT–PCR as described[22]. Briefly, RNA isolated using the Tryzol reagent (Gibco-BRL) was treated with DNase in three sequential steps, reaching a final volume of 20 μl. After the last treatment, 1-μl aliquots were amplified by PCR using degenerate primers to *vir* subfamilies *A* and *C* and *Pvstp1*. Only RNA preparations that did not amplify any products, and so were free of contaminating genomic *P. vivax* DNA, were used for further analysis. RNA was reverse transcribed using random hexanucleotide primers (Perkin Elmer) and analysed by PCR using degenerate oligonucleotides to *vir* subfamilies. We used annealing temperatures 5 °C below the calculated T_m value of the primer pairs. The resulting PCR products were examined by Southern analysis and sequenced.

GST–VIR-C fusion proteins

vir gene tags containing exon 2 were cloned into pGEX-3X (Pharmacia), expressed in *Escherichia coli* and the resulting GST fusion proteins affinity purified, according to the manufacturer's instructions. Purified proteins were examined by western blot analysis and enzyme-linked immunoabsorbent assays, using immune sera from different *P. vivax* patients, as described[23].

Laser confocal scanning microscopy

VIR-C-specific antibodies were affinity purified from the serum of *P. vivax* patient 40 using GST–VIR-C1-29 as the ligand, as decribed[24]. The mouse polyclonal anti *P. vivax* MSP-1 has been described[25]. A guinea-pig antiserum to a semi-conserved amino-acid motif (RKNFKNTYAKKKGLK) in VIR subfamily D was purchased from Eurogentec. We obtained reticulocytes infected with *P. vivax* schizonts from *P. vivax* patients, and fixed them on glass slides as described[26]. Fluorescein isothiocyanate (FITC)-conjugated affinity-purified $F(ab')_2$ fragment donkey anti-human IgG + IgM (H+L), Cy3-conjugated affinity-purified donkey anti-mouse IgG (H+L), and FITC-conjugated affinity-purified donkey anti guinea pig IgG (H+L) were purchased from Dianova and used according to the manufacturer's instructions. Hoechst 33342 was purchased from Sigma. Immunofluorescence signals were monitored using the LSM 510 (Zeiss).

Data release

The fully annotated sequence of IVD10 (accession number AL360354) is available from http://www.sanger.ac.uk/Projects/P_vivax. The accession numbers for the expressed *vir* gene tags are AF314564 to AF314568, the last corresponding to *vir-C1-29*.

Received 6 November 2000; accepted 27 January 2001.

1. David, P. H., del Portillo, H. A. & Mendis, K. N. *Plasmodium vivax* malaria: parasite biology defines potential targets for vaccine development. *Biol. Cell* **64,** 251–260 (1988).
2. Galinski, M. R. & Barnwell, J. W. *Plasmodium vivax*: merozoites, invasion of reticulocytes and considerations for malaria vaccine development. *Parasitol. Today* **12,** 20–29 (1996).
3. Baruch, D. I. *et al.* Cloning of the *P. falciparum* gene encoding PfEMP1, a malarial *var*iant antigen and adherence receptor on the surface of parasitized human erythrocytes. *Cell* **82,** 77–87 (1995).
4. Smith, J. D. *et al.* Switches in expression of *Plasmodium falciparum var* genes correlate with changes in antigenic and cytoadherent phenotypes of infected erythrocytes. *Cell* **82,** 101–110 (1995).
5. Su, X. *et al.* The large diverse gene family *var* encodes proteins involved in cytoadherence and antigenic *var*iation of *Plasmodium falciparum*-infected erythrocytes. *Cell* **82,** 89–100 (1995).
6. Kyes, S. Rowe, A. J., Kriek, N. & Newbold, C. I. Rifins: a second family of clonally variant proteins expressed on the surface of red cells infected with *Plasmodium falciparum*. *Proc. Natl Acad. Sci. USA* **96,** 9333–9338 (1999).
7. Fernandez, V., Hommel, M., Chen, Q., Hagblom, P. & Wahlgren, M. Small, clonally variant antigens expressed on the surface of *Plasmodium falciparum*-infected erythrocyte are encoded by the *rif* gene family and are the target of human immune responses. *J. Exp. Med.* **190,** 1393–1403 (1999).
8. Cheng, Q. *et al. stevor* and *rif* are *Plasmodium falciparum* multicopy gene families which potentially encode variant antigens. *Mol. Biochem. Parasitol.* **97,** 161–176 (1998).
9. Golenda, C. F., Li, J. & Rosenberg, R. Continuous *in vitro* propagation of the malaria parasite *Plasmodium vivax*. *Proc. Natl Acad. Sci. USA* **94,** 6786–6791 (1997).
10. Camargo, A. A., Fischer, K., Lanzer, M. & del Portillo, H. A. Construction and characterization of a *Plasmodium vivax* genomic library in yeast artificial chromosomes. *Genomics* **42,** 467–473 (1997).
11. Ponzi, M., Pace, T., Dore, F. & Frontali, C. Identification of a telomeric DNA sequence in *Plasmodium berghei*. *EMBO J.* **4,** 2991–2995 (1985).
12. Vernick, K. D. & McCutchan, T. F. Sequence and structure of a *Plasmodium falciparum* telomere. *Mol. Biochem. Parasitol.* **28,** 85–94 (1988).
13. McCutchan, T. F., Dame, J. B., Miller, L. H. & Barnwell, J. Evolutionary relatedness of *Plasmodium* species as determined by the structure of DNA. *Science* **225,** 808–811 (1984).
14. Gardner, M. J. *et al.* Chromosome 2 sequence of the human malaria parasite *Plasmodium falciparum*. *Science* **282,** 1126–1132 (1998).
15. Bowman, S. *et al.* The complete nucleotide sequence of chromosome 3 of *Plasmodium falciparum*. *Nature* **400,** 532–538 (1999).
16. The *C. elegans* sequencing consortium. Genome sequence of the nematode *C. elegans*: a platform for investigating biology. *Science* **282,** 2012–2018 (1998).
17. Al-Khedery, B., Barnwell, J. W. & Galinski, M. R. Antigenic variation in malaria: a 3′ genomic alteration associated with the expression of a *P. knowlesi* variant antigen. *Mol. Cell* **3,** 131–141 (1999).
18. Persson, B. Bioinformatics in protein analysis. *EXS* **88,** 215–131 (2000).
19. Mendis, K. N., Ihalamulla, R. I. & David, P. H. Diversity of *Plasmodium vivax*-induced antigens on the surface of infected human erythrocytes. *Am. J. Trop. Med. Hyg.* **38,** 42–46 (1988).
20. Freitas-Junior, L. H. *et al.* Frequent ectopic recombination of virulence factor genes in telomeric chromosome clusters of *P. falciparum*. *Nature* **407,** 1018–1022 (2000).
21. Vaudin, M. *et al.* The construction and analysis of M13 libraries prepared from YAC DNA. *Nucleic Acids Res.* **23,** 670–674 (1995).
22. Kyes, S., Pinches, R. & Newbold, C. A simple RNA analysis method shows *var* and *rif* multigene family expression patterns in *Plasmodium falciparum*. *Mol Biochem. Parasitol.* **105,** 311–315 (2000).
23. Levitus, G. *et al.* Characterization of naturally acquired human IgG responses against the N-terminal region of the merozoite surface protein 1 of *Plasmodium* vivax. *Am. J. Trop. Med. Hyg.* **51,** 68–76 (1994).
24. Hall, R. *et al.* Major surface antigen gene of a human malaria parasite cloned and expressed in bacteria. *Nature* **311,** 379–382 (1984).
25. Oliveira, C. I. *et al.* Antigenic properties of the Merozoite Surface Protein 1 gene of *Plasmodium vivax*. *Vaccine* **17,** 2959–2968 (1999).
26. Voller, A. & O'Neill, P. O. Immunofluorescence method suitable for large scale application to malaria. *Bull. World Health Organ.* **45,** 524–529 (1971).

Acknowledgements

We thank all the patients who participated in this study; J. d'Arc Neves for collecting blood samples; A. Craig for helping in the initial liasion with the Sanger Centre; M. Quail and the subcloning group; members of team 23 and other members of the Pathogen Unit at the Sanger Centre for their help in sequence generation and analysis; N. Hall for the creation of the web pages; Y. Cully for the graphics; and H. Bujard for encouragement throughout this work. This work was supported by the the Deutsche Forschungsgemeinschaft (to M.L.) and the European Commission (to M.L. and H.A.P.).

Correspondence and requests for materials should be addressed to H.A.P. (e-mail: hernando@icb.usp.br).

The ATM–Chk2–Cdc25A checkpoint pathway guards against radioresistant DNA synthesis

Jacob Falck, Niels Mailand, Randi G. Syljuåsen, Jiri Bartek & Jiri Lukas

Institute of Cancer Biology, Danish Cancer Society, Strandboulevarden 49, DK-2100 Copenhagen, Denmark

When exposed to ionizing radiation (IR), eukaryotic cells activate checkpoint pathways to delay the progression of the cell cycle[1–3]. Defects in the IR-induced S-phase checkpoint cause 'radioresistant DNA synthesis', a phenomenon that has been identified in cancer-prone patients suffering from ataxia-telangiectasia, a disease caused by mutations in the ATM gene[4–6]. The Cdc25A phosphatase[7] activates the cyclin-dependent kinase 2 (Cdk2) needed for DNA synthesis[8,9], but becomes degraded in response to DNA damage[10] or stalled replication[11]. Here we report a functional link between ATM, the checkpoint signalling kinase Chk2/Cds1 (Chk2)[12] and Cdc25A, and implicate this mechanism

in controlling the S-phase checkpoint. We show that IR-induced destruction of Cdc25A requires both ATM and the Chk2-mediated phosphorylation of Cdc25A on serine 123. An IR-induced loss of Cdc25A protein prevents dephosphorylation of Cdk2 and leads to a transient blockade of DNA replication. We also show that tumour-associated Chk2 alleles[13] cannot bind or phosphorylate Cdc25A, and that cells expressing these Chk2 alleles, elevated Cdc25A or a Cdk2 mutant unable to undergo inhibitory phosphorylation (Cdk2AF) fail to inhibit DNA synthesis when irradiated. These results support Chk2 as a candidate tumour suppressor, and identify the ATM–Chk2–Cdc25A–Cdk2 pathway as a genomic integrity checkpoint that prevents radioresistant DNA synthesis.

To investigate whether degradation of Cdc25A affects the IR-induced S-phase checkpoint, we measured DNA synthesis in human U-2-OS/B3C4 cells engineered to express ectopic haemagglutinin A (HA)-tagged Cdc25A in a tetracycline-repressible manner[10]. Endogenous Cdc25A was degraded rapidly in response to IR, along with the dose-dependent inhibition of DNA synthesis (Fig. 1a); however, when the HA–Cdc25A protein was transiently elevated to levels high enough to prevent its degradation, it abrogated the S-phase checkpoint (Fig. 1a), resulting in radioresistant DNA synthesis (RDS) comparable to that seen in cells from ataxia-telangiectasia patients[4–6].

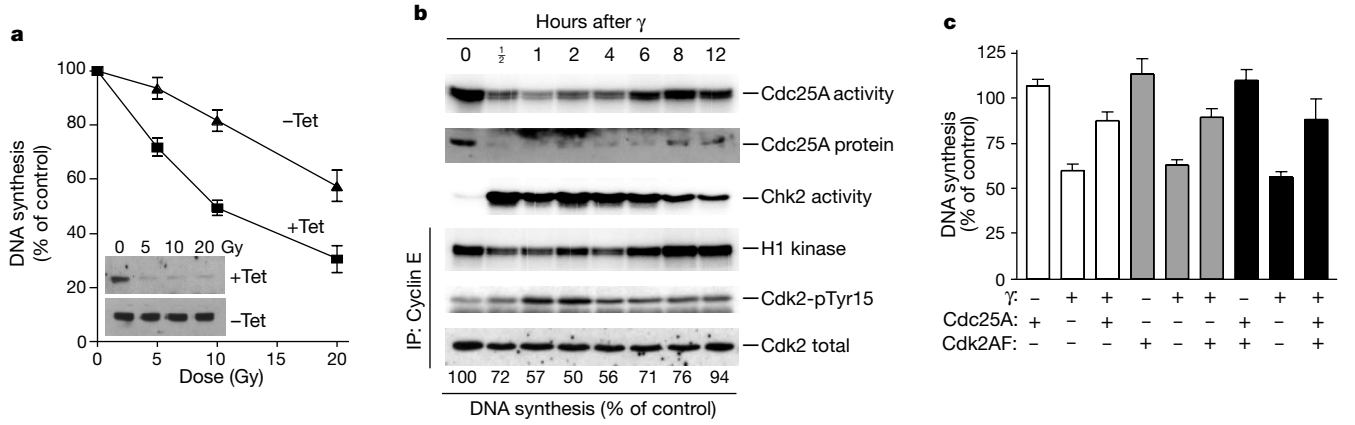

Figure 1 Effects and regulation of IR-induced destruction of Cdc25A. **a**, DNA synthesis and Cdc25A abundance (inset) in γ-irradiated U-2-OS/B3C4 cells repressed (+Tet) or induced (–Tet) 1 h before IR to express ectopic HA–Cdc25A. **b**, Kinetics of IR-induced activities, and abundance of Cdc25A and Chk2, cyclin-E-associated H1 kinase activity and Cdk2 Tyr 15 phosphorylation in U-2-OS cells exposed to 10 Gy. **c**, DNA synthesis in untreated or 10-Gy γ-irradiated CD20-sorted U-2-OS/T-Rex cells expressing Cdc25A and/or Cdk2AF.

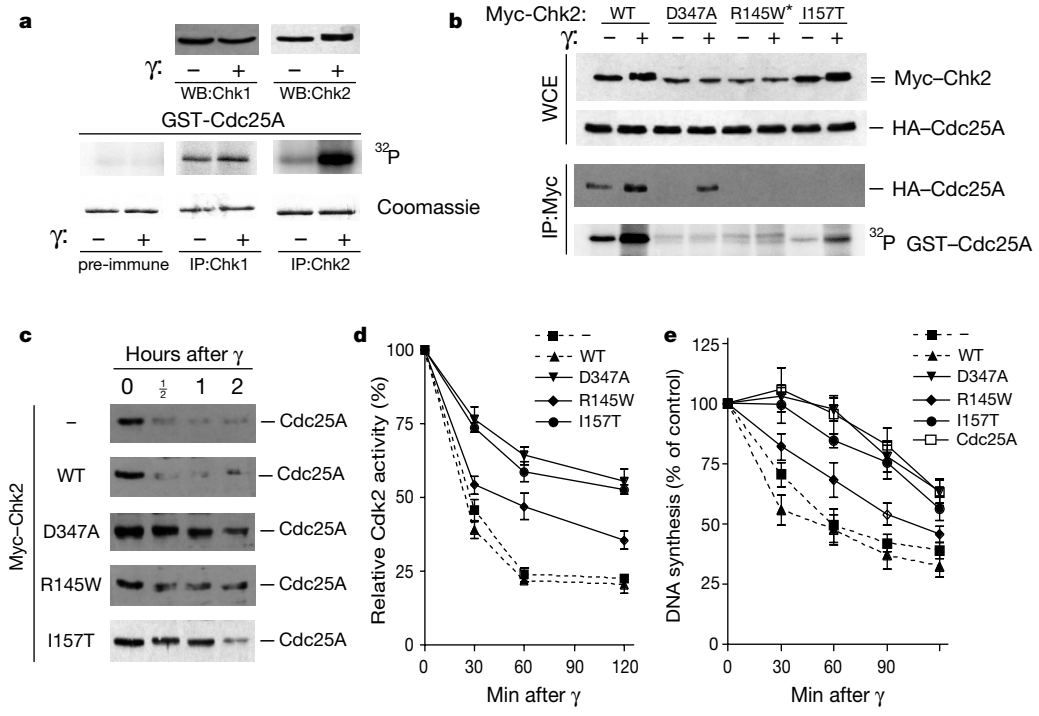

Figure 2 Failure of Chk2 mutants to bind and induce degradation of Cdc25A abrogates the S-phase checkpoint. **a**, Immunoblots of Chk1 and Chk2 and their kinase activities towards GST–Cdc25A in untreated (–) or 10-Gy γ-irradiated (+) U-2-OS cells. **b**, Top, U-2-OS/B3C4 cells were transfected with Myc–Chk2 plasmids as indicated, stimulated to express HA–Cdc25A for 3 h, γ-irradiated (10 Gy; +) or left untreated (–), and immunoblotted for Myc–Chk2 and Cdc25A (WCE, whole-cell extract). Bottom, anti-Myc immunoprecipitates were assayed for co-precipitated Cdc25A and for *in vitro* kinase activity towards GST–Cdc25A (bottom). Asterisk, a threefold excess of Myc–Chk2-R145W was transfected. **c**, **d**, Various U-2-OS/Myc–Chk2 clones were analysed for Cdc25A abundance (**c**) and Cdk2-associated kinase activity (**d**) at the indicated time points after γ-irradiation (10 Gy). **e**, DNA synthesis in various U-2-OS/Myc–Chk2 clones measured after γ-irradiation (10 Gy). Open squares, U-2-OS/B3C4 cells with induced Cdc25A.

We thought that if destruction of Cdc25A were involved in the S-phase checkpoint, it should be only transient, as the IR-induced inhibition of DNA replication lasts only several hours[5]. Our kinetic measurements showed that Cdc25A was almost completely downregulated by 30 min after irradiation, and recovered to the levels of non-irradiated cells 4–8 h later (Fig. 1b). The maximum downregulation of Cdc25A between 1 and 3 h after IR correlated with an increased inhibitory phosphorylation of Cdk2 on Tyr 15, a reduction of the S-phase-promoting cyclin E/Cdk2 kinase activity, and nearly 50% inhibition of DNA synthesis (Fig. 1b).

These results suggested that the main consequence of the IR-induced Cdc25A downregulation was inhibition of Cdk2, implying that interference with the Cdk2 inhibitory phosphorylation should abrogate the S-phase checkpoint. Indeed, brief conditional expression of the Cdk2AF allele[14], in which the inhibitory Thr 14 and Tyr 15 are replaced by alanine and phenylalanine, respectively, mimicked the effect of Cdc25A overexpression and resulted in RDS (Fig. 1c). Simultaneous expression of both HA–Cdc25A and Cdk2AF did not further increase the degree of RDS (Fig. 1c), indicating that both proteins function in the same pathway.

Ultraviolet-light-induced downregulation of Cdc25A requires the activation of Chk1 (ref. 10), a key signal transducer that, together with Chk2, is implicated in checkpoint pathways activated by damaged or unreplicated DNA[12,15–19]. To assess whether Chk1 or Chk2 may regulate abundance of Cdc25A on IR, we measured their ability to phosphorylate Cdc25A. The activity and electrophoretic mobility of Chk1 remained unchanged until several hours after IR (Fig. 2a; and data not shown), but Chk2 became activated rapidly, as judged by its lower electrophoretic mobility and enhanced phosphorylation of GST–Cdc25A 1 h after IR (Fig. 2a). These results suggest that Chk2, but not Chk1, becomes activated with kinetics indicative of a link between IR-induced DNA damage and the rapid inhibition of S phase. Detailed time-course measurements showed that the kinetics of IR-induced Chk2 activity closely paralleled the loss of Cdc25A protein and phosphatase activity, the downregulation of cyclin E/Cdk2 by inhibitory phosphorylation, and the decrease in DNA synthesis (Fig. 1b).

To gain mechanistic insight into this link between Chk2 and Cdc25A, we assessed the IR responsiveness of Myc-tagged forms of human Chk2 transiently transfected into U-2-OS/B3C4 cells, including the engineered catalytically inactive D347A mutant[12,20], and the R145W and I157T alleles[13] with mutations in the putative protein-interaction FHA domain[12,21,22], identified in sporadic colon cancer and as a germ-line mutation in the cancer-prone Li–Fraumeni syndrome, respectively[13]. On exposure to IR, the ectopic wild-type Chk2 became rapidly shifted into a more slowly migrating form, and increased its ability to interact physically with transiently elevated HA–Cdc25A *in vivo* and phosphorylate GST–Cdc25A *in vitro* (Fig. 2b). In contrast, basal activities of the three mutants of Chk2 were barely detectable in non-irradiated cells and remained low even after exposure to IR (Fig. 2b).

Notably, the D347A mutant still bound HA–Cdc25A after IR (Fig. 2b), implying that the interaction of Chk2 with its substrate(s) is mediated through its modification by an upstream regulator, independently of Chk2 autocatalytic activity. In contrast, the R145W and I157T cancer-associated mutants of Chk2 could not

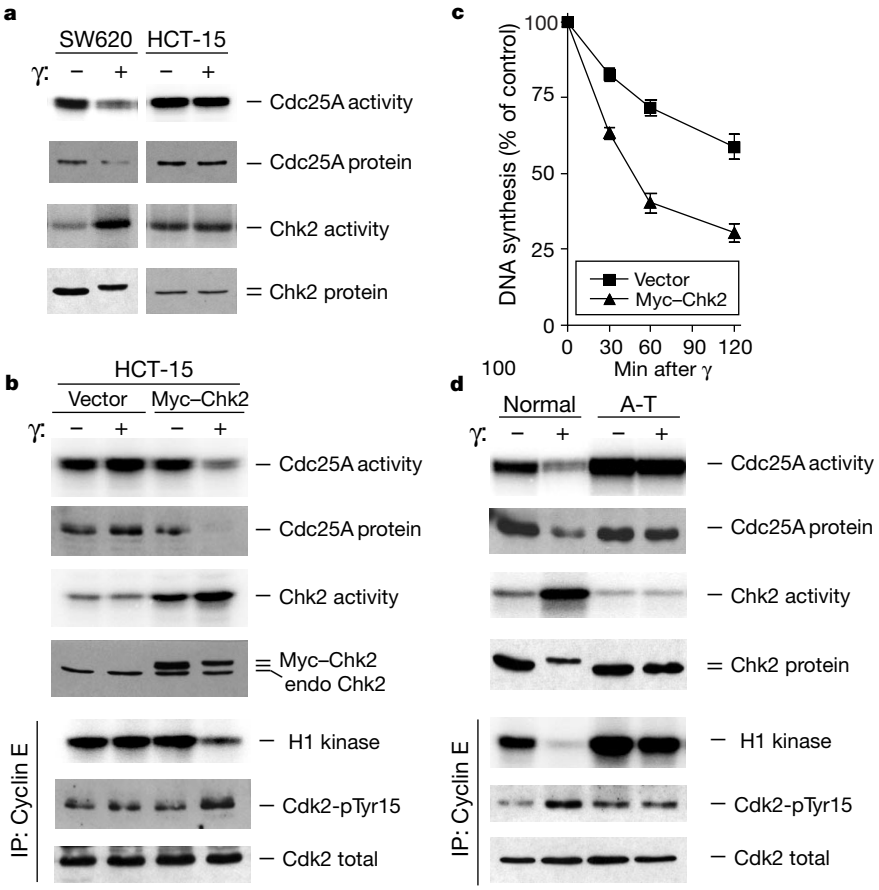

Figure 3 IR-induced destruction of Cdc25A requires functional ATM and Chk2. **a**, Abundance and activities of Cdc25A and Chk2 in untreated (–) or γ-irradiated (10 Gy; +) SW620 and HCT-15 cells . **b**, HCT-15-derived cells were γ-irradiated (10 Gy; +) or left untreated (–) and analysed for activities and abundance of Cdc25A and Chk2, cyclin-E-associated H1 kinase activity, and Cdk2 levels (Tyr 15 phosphorylated and total). **c**, DNA synthesis in control vector versus Chk2-reconsitituted (Myc–Chk2) HCT-15 cells measured after IR (10 Gy). **d**, Normal or ataxia-telangiectasia (A-T) lymphoblasts were treated and analysed as in **b**.

bind HA–Cdc25A, even though the I157T mutant preserved the IR-induced mobility shift (Fig. 2b). Thus, the tumour-associated Chk2 proteins seem defective in their ability to bind and phosphorylate substrates such as Cdc25A.

To examine whether Chk2 and Cdc25A function in a common pathway, we transfected U-2-OS cells with plasmids encoding the Chk2 alleles described in Fig. 2b, together with a gene coding for puromycin resistance. Whereas puromycin-resistant cell populations transfected with wild-type Chk2 or empty plasmid efficiently degraded Cdc25A when exposed to IR (Fig. 2c), cells expressing any of the Chk2 mutants retained substantial amounts of Cdc25A when irradiated (Fig. 2c). Consistent with these differential abilities to modulate Cdc25A protein levels, Cdk2 activity declined in cells transfected with empty vector or wild-type Chk2, but remained elevated in cells expressing the Chk2 mutants (Fig. 2d). Consequently, whereas the control cells responded by inhibiting DNA synthesis, cells expressing the Chk2 mutants failed to impose the S-phase blockade and exhibited RDS comparable to that of cells conditionally overexpressing Cdc25A (Fig. 2e). Thus, Chk2 alleles defective in catalytic activity or interaction with Cdc25A behaved as dominant-negative mutants that abrogated the S-phase checkpoint, which is consistent with Chk2 operating upstream of Cdc25A and Cdk2 in a common pathway.

In addition to Cdc25A, Chk2 also efficiently phosphorylates the p53 tumour suppressor in response to DNA damage[20,23]; however, the former substrate seems more relevant for S-phase arrest induced by IR, as p53 controls the G1 and sustains the G2/M checkpoints, rather than the S-phase checkpoint[24–26], and RDS occurs independently of p53 status[27]. Consistent with this, rapid degradation of Cdc25A and loss of its phosphatase activity occurred in SW620 (wild-type for Chk2) but not in HCT-15 cells expressing mutant Chk2 after exposure to IR (ref. 13; Fig. 3a). Notably, both of these colon cancer cell lines express mutant p53 (ref. 13). Re-introduction of wild-type Chk2 into HCT-15 cells to a level exceeding that of the endogenous mutated protein restored the S-phase checkpoint response, including degradation of Cdc25A, increased inhibitory phosphorylation of Cdk2 and downregulation of cyclin E/Cdk2 kinase activity (Fig. 3b), and the ability to arrest S-phase progression (Fig. 3c). These results further support Chk2 as a mediator for rapidly destructing Cdc25A in response to IR, in a p53-independent S-phase checkpoint that protects cells against RDS.

As RDS occurs in cells with a defective ATM gene[4–6], as well as through deregulation of Chk2 or Cdc25A, and as ATM activates Chk2 directly (ref. 12), we next compared the response of the Chk2–Cdc25A–Cdk2 pathway in lymphoblasts derived from ataxia-telangiectasia patients to those isolated from normal individuals. Unlike normal lymphoblasts, irradiated ataxia-telangiectasia cells were unable to activate Chk2 and downregulate Cdc25A protein and activity (Fig. 3d). Consequently, exposure of ataxia-telangiectasia lymphoblasts to IR caused neither an increase in Cdk2 Tyr 15 phosphorylation nor an inhibition of cyclin E/Cdk2 kinase activity (Fig. 3d), which is consistent with the well-documented RDS phenotype in these cells[5].

As signals from damaged DNA are often propagated through

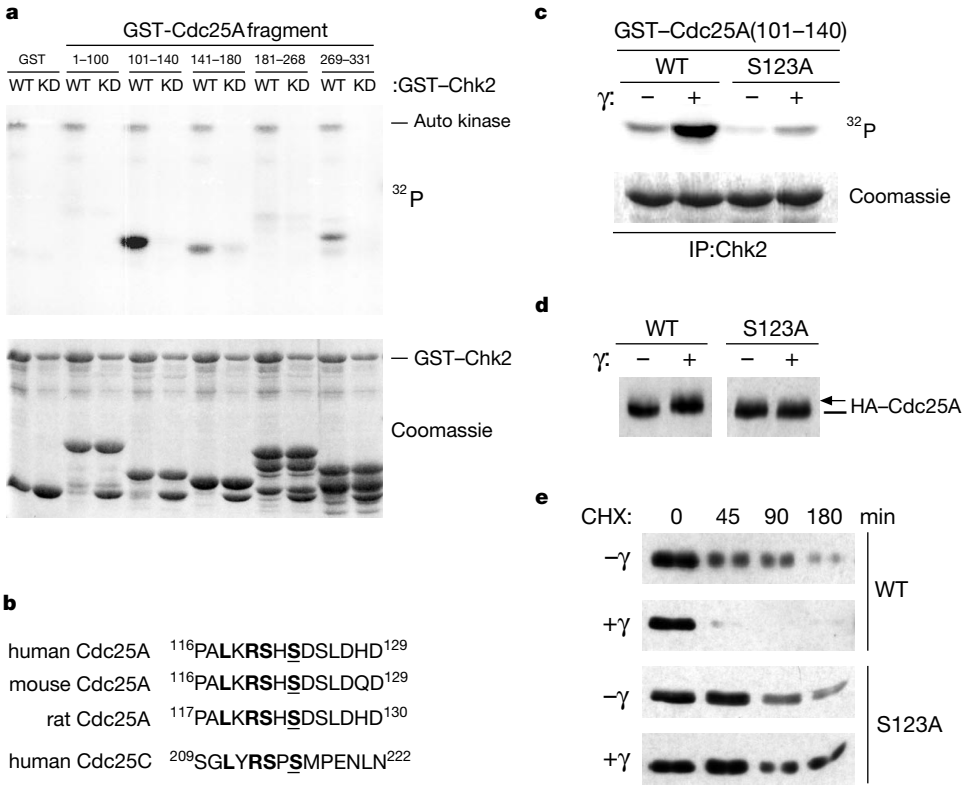

Figure 4 Chk2 phosphorylates Cdc25A on Ser 123 and triggers its IR-induced destruction. **a**, GST–Cdc25A fragments were incubated with purified wild type (WT) or catalytically inactive (KD) GST–Chk2. Proteins resolved by SDS–PAGE were visualized by autoradiography (top) or Coomassie staining (bottom). **b**, Amino-acid sequence flanking Ser 123 in human, mouse and rat Cdc25A, aligned with the Chk1/2-phosphorylated region of human Cdc25C. **c**, GST–Cdc25A(101–140) (WT) or GST–Cdc25A(101–140) (S123A) was incubated with Chk2 immunoprecipitates from untreated (–) or 10-Gy γ-irradiated (+) U-2-OS cells. Proteins were resolved and visualized as in **b**. **d**, U-2-OS cells transiently transfected with WT or S123A HA–Cdc25A were γ-irradiated (10 Gy; +) or left untreated (–) in the presence of proteasome inhibitor LLnL to prevent destruction, and cell lysates were analysed by immunoblotting. Arrow indicates IR-induced slower-migrating form of Cdc25A. **e**, U-2-OS cells transfected with WT or S123A HA–Cdc25A were γ-irradiated (10 Gy; +) or not (–) 12 h after transfection, incubated with cycloheximide (CHX; 25 μg ml^{-1}) and immunoblotted for HA–Cdc25A at the indicated times after CHX addition.

phosphorylation cascades, we next identified the Cdc25A residue(s) directly phosphorylated by Chk2, presumably to prime Cdc25A for rapid destruction after IR-induced DNA damage. We made glutathione *S*-transferase (GST)-coupled fragments derived from the Cdc25A regulatory domain and subjected them to phosphorylation by purified GST–Chk2. The fragment spanning amino acids 101–140 was strongly phosphorylated by wild-type but not by catalytically inactive Chk2 (Fig. 4a), and the sequence flanking Ser 123 of human Cdc25A, conserved in diverse mammalian species, matched the criteria for a Chk2/Chk1 consensus site identified in other proteins such as Cdc25C[12,16–18] (Fig. 4b). Replacement of Ser 123 with alanine abolished the ability of the IR-activated Chk2 to phosphorylate the corresponding GST–Cdc25A fragment (Fig. 4c). The S123A mutation in the context of full-length Cdc25A resulted in a protein that, unlike wild-type Cdc25A, did not undergo an IR-induced shift when separated on an SDS gel (Fig. 4d), indicating that *in vivo* the S123A substitution abolished an important IR-dependent modification of Cdc25A. Significantly, the S123A mutation rendered Cdc25A resistant to IR-induced degradation under conditions in which a comparable amount of moderately overexpressed wild-type Cdc25A was still effectively degraded *in vivo* (Fig. 4e). We conclude that Chk2-dependent phosphorylation of Cdc25A on Ser 123 represents a critical step in promoting its rapid destruction in response to IR-induced DNA damage.

On the basis of this study, we propose that the ATM–Chk2–Cdc25A–Cdk2 pathway may provide the molecular explanation of the defence mechanism protecting human cells against RDS. The key components and events along this pathway in cells proficient in the S-phase checkpoint are outlined in Fig. 5 (left). The biological and pathophysiological relevance of this mechanism is further supported by the fact that tumour-associated defects of any of its main components cause RDS (Fig. 5, right), and may predispose to, or promote, tumorigenesis (refs 5, 13, 28; and this study). Cells undergoing DNA replication are particularly vulnerable to genotoxic stress including IR; the rapid degradation of Cdc25A and subsequent silencing of the Cdk2 activity may represent the initial defence barrier, which inhibits DNA synthesis to allow efficient repair. Cdc25A extends the list of important checkpoint mediators targeted by Chk2, currently encompassing the mitotic activator Cdc25C[12], and the p53 (refs 20, 23) and BRCA1 (ref. 29) tumour suppressors, thereby implicating Chk2 in a complex network controlling G1, S and G2/M checkpoints, as well as DNA repair. Such a central role in protecting genome integrity is also consistent with the proposed candidacy of Chk2 for a new tumour suppressor, whose mutations may predispose to tumorigenesis in diverse tissues, as seen in patients with Li–Fraumeni syndrome[13]. Our finding that the tumour-associated Chk2 alleles are indeed loss-of-function mutants provides the missing functional evidence indicating that Chk2 is a genuine tumour suppressor. □

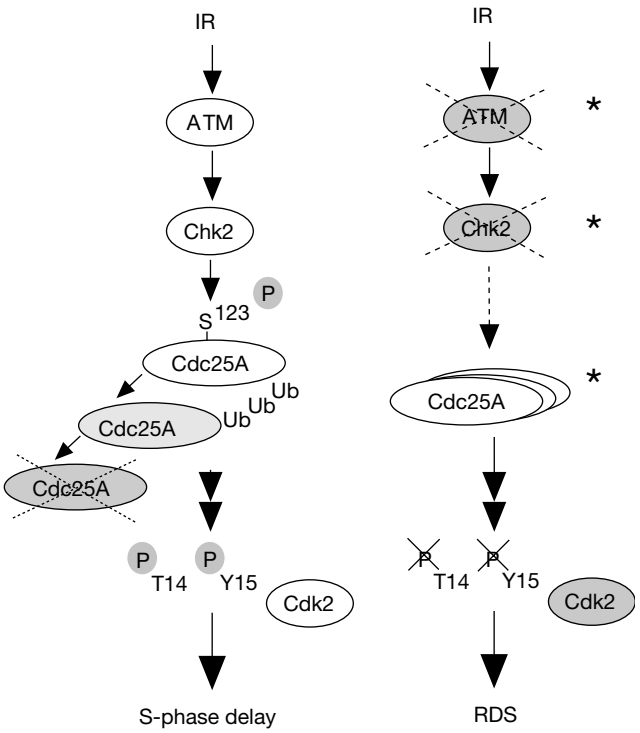

Figure 5 Model of the IR-induced S-phase checkpoint pathway in normal (left) versus checkpoint-deficient (right) cells. Pathway components targeted in cancer are marked by an asterisk. Ub, ubiqitin chains.

Methods

Antibodies and immunochemistry

Mouse antibody HE172 to cyclin E, as well as immunoblotting, immunoprecipitation, Cdc25A phosphatase activity and *in vitro* kinase assays have been described[10]. Rabbit antisera to Cdk2 (M2) and Chk1 (FL-476), and mouse antibody to Cdc25A (F-6, used to detect the endogenous protein) were from Santa Cruz. Rabbit antiserum to Tyr15-phosphorylated Cdk1/Cdk2 was from Calbiochem, and mouse monoclonal antibody to CD20 was from Becton Dickinson. The 9E10 antibody to the Myc epitope was a gift from G. Evan. We generated mouse monoclonal antibodies to human Chk2 (DCS-270) and Cdc25A (DCS-127) by standard hybridoma technology.

Plasmids

To construct the Myc-tagged Chk2 expression vector, the human Chk2 complementary DNA (a gift from S. Elledge) was amplified by PCR with *Pfu* polymerase (Stratagene) and cloned into a pcDNA3 vector (Invitrogen) containing a Myc tag. The catalytically inactive D347A[12,20], and tumour-associated R145W[13] and I157T[13] mutants of Chk2, as well as the Cdc25A S123A mutant were generated using the QuikChange Site-Directed Mutagenesis kit (Stratagene). We expressed and purified GST–Chk2 and GST–Cdc25A[10] (full length and fragments) according to standard procedures.

Cell culture and RDS assay

We grew U-2-OS cells[10] and SW-620 cells in DMEM containing 10% fetal bovine serum (FBS). HCT-15 cells[13] and lymphoblasts derived from normal and ataxia-telangiectasia patients (donated by Y. Shiloh) were grown in RPMI with 10% FBS. The U-2-OS-derived B3C4 clone conditionally expressing haemagglutinin (HA)-tagged Cdc25A has been described[10]. Expression of the transgene was induced by culturing the cells in tetracycline-free medium for the durations specified in the figure legends. The U-2-OS-derived T-Rex cell line was from Invitrogen. We induced expression of Cdc25A and Cdk2AF by adding tetracycline (1 $\mu g\,ml^{-1}$) 4 h before irradiation (Fig. 1c); ectopic CD20 was expressed throughout the experiment. Isolation of CD20-positive U-2-OS/T-Rex cells with anti-CD20-coupled Dynabeads has been described[30]. The U-2-OS- and HCT-15-derived polyclonal cell lines stably expressing Myc-tagged wild-type or mutant Chk2 were generated by calcium phosphate transfection (U-2-OS) or electroporation (HCT-15) of cells with empty pcDNA3–Myc vector or pcDNA3–Myc vector containing wild-type or mutant Chk2. A vector encoding puromycin resistance (pBabe-puro) was co-transfected, the cells were selected for neomycin (G418; 400 $\mu g\,ml^{-1}$) and puromycin (1 $\mu g\,ml^{-1}$) resistance, and pooled when visible colonies emerged. Ionizing radiation was delivered by X-ray generator (RT100, Philips Medico; 100 kV, 8 mA, dose-rate 0.92 Gy min^{-1}), and cell extracts were prepared 1 h later except where indicated otherwise. Inhibition of DNA synthesis and RDS after ionizing radiation were monitored as described[6,26].

Received 16 November 2000; accepted 11 January 2001.

1. Weinert, T. DNA damage and checkpoint pathways: molecular anatomy and interactions with repair. *Cell* **94,** 555–558 (1998).
2. Hartwell, L. H. & Kastan, M. B. Cell cycle control and cancer. *Science* **266,** 1821–1828 (1994).
3. Elledge, S. J. Cell cycle checkpoints: preventing an identity crisis. *Science* **274,** 1664–1672 (1996).
4. Painter, R. B. & Young, B. R. Radiosensitivity in ataxia-telangiectasia: a new explanation. *Proc. Natl Acad. Sci. USA* **77,** 7315–7317 (1980).
5. Rotman, G. & Shiloh, Y. ATM: a mediator of multiple responses to genotoxic stress. *Oncogene* **18,** 6135–6144 (1999).
6. Stewart, G. S. *et al.* The DNA double-strand break repair gene hMRE11 is mutated in individuals with an ataxia-telangiectasia-like disorder. *Cell* **99,** 577–587 (1999).
7. Galaktionov, K. & Beach, D. Specific activation of cdc25 tyrosine phosphatases by B-type cyclins: evidence for multiple roles of mitotic cyclins. *Cell* **67,** 1181–1194 (1991).
8. Hoffmann, I., Draetta, G. & Karsenti, E. Activation of the phosphatase activity of human cdc25A by a cdk2-cyclin E dependent phosphorylation at the G1/S transition. *EMBO J.* **13,** 4302–4310 (1994).
9. Jinno, S. *et al.* Cdc25A is a novel phosphatase functioning early in the cell cycle. *EMBO J.* **13,** 1549–1556 (1994).
10. Mailand, N. *et al.* Rapid destruction of Cdc25A in response to DNA damage. *Science* **288,** 1425–1429 (2000).
11. Molinari, M. *et al.* Human Cdc25A inactivation in response to S phase inhibition and its role in preventing premature mitosis. *EMBO Reps* **1,** 71–79 (2000).

12. Matsuoka, S., Huang, M. & Elledge, S. J. Linkage of ATM to cell cycle regulation by the Chk2 protein kinase. *Science* **282,** 1893–1897 (1998).
13. Bell, D. W. *et al.* Heterozygous germ line hCHK2 mutations in Li–Fraumeni syndrome. *Science* **286,** 2528–2531 (1999).
14. Gu, Y., Rosenblatt J. & Morgan, D. O. Cell cycle regulation of CDK2 activity by phosphorylation of Thr160 and Tyr15. *EMBO J.* **11,** 3995–4005 (1992).
15. Boddy, M. N., Furnari, B., Mondesert, O. & Russell, P. Replication checkpoint enforced by kinases Cds1 and Chk1. *Science* **280,** 909–912 (1998).
16. Furnari, B., Rhind, N. & Russell, P. Cdc25 mitotic inducer targeted by chk1 DNA damage checkpoint kinase. *Science* **277,** 1495–1497 (1997).
17. Peng, C. Y. *et al.* Mitotic and G2 checkpoint control: regulation of 14-3-3 protein binding by phosphorylation of Cdc25C on serine-216. *Science* **277,** 1501–1505 (1997).
18. Sanchez, Y. *et al.* Conservation of the Chk1 checkpoint pathway in mammals: linkage of DNA damage to Cdk regulation through Cdc25. *Science* **277,** 1497–1501 (1997).
19. Zeng, Y. *et al.* Replication checkpoint requires phosphorylation of the phosphatase Cdc25 by Cds1 or Chk1. *Nature* **395,** 507–510 (1998).
20. Chehab, N. H., Malikzay, A., Appel, M. & Halazonetis, T. D. Chk2/hCds1 functions as a DNA damage checkpoint in G_1 by stabilizing p53. *Genes Dev.* **14,** 278–288 (2000).
21. Sun, Z., Hsiao, J., Fay, D. S. & Stern, D. F. Rad 53 FHA domain associated with phosphorylated Rad9 in the DNA damage checkpoint. *Science* **281,** 272–274 (1998).
22. Durocher, D., Henckel, J., Fersht, A. R. & Jackson, S. P. The FHA domain is a modular phosphopeptide recognition motif. *Mol. Cell* **4,** 387–394 (1999).
23. Hirao, A. *et al.* DNA damage-induced activation of p53 by the checkpoint kinase Chk2. *Science* **287,** 1824–1827 (2000).
24. Chan, T. A., Hermeking, H., Lengauer, C., Kinzler, K. W. & Vogelstein, B. 14-3-3σ is required to prevent mitotic catastrophe after DNA damage. *Nature* **401,** 616–620 (1999).
25. Giaccia, A. J. & Kastan, M. B. The complexity of p53 modulation: emerging patterns from divergent signals. *Genes Dev.* **12,** 2973–2983 (1998).
26. Lim, D. S. *et al.* ATM phosphorylates p95/nbs1 in an S-phase checkpoint pathway. *Nature* **404,** 613–617 (2000).
27. Xie, G. *et al.* Requirements for p53 and ATM gene product in the regulation of G1/S and S phase checkpoints. *Oncogene* **16,** 721–736 (1998).
28. Galaktionov, K. *et al.* CDC25 phosphatases as potential human oncogenes. *Science* **269,** 1575–1577 (1995).
29. Lee, J. S., Collins, K. M., Brown, A. L., Lee, C. H. & Chung, J. H. hCds1-mediated phosphorylation of BRCA1 regulates the DNA damage response. *Nature* **404,** 201–204 (2000).
30. Santoni-Rugiu, E., Falck, J., Mailand, N., Bartek, J & Lukas, J. Involvement of Myc activity in a G1/S-promoting mechanism parallel to the pRb/E2F pathway. *Mol. Cell. Biol.* **20,** 3497–3509 (2000).

Acknowledgements

We thank S. Elledge, G. Evan, S. I. Reed and Y. Shiloh for providing reagents; K. Hansen for advice; and the Danish Cancer Society, the Human Frontier Science Programme, Alfred Benzon's Fund, the European Commission, the Danish Medical Research Council and the Danish Cancer Research Fund for financial support.

Correspondence and requests for materials should be addressed to J.B. (e-mail: bartek@biobase.dk).

correction

arrow encodes an LDL-receptor-related protein essential for Wingless signalling

Marcel Wehrli, Scott T. Dougan, Kim Caldwell, Louise O'Keefe, Stephanie Schwartz, Dalit Vaizel-Ohayon, Eyal Schejter, Andrew Tomlinson & Stephen DiNardo

Nature **407,** 527–530 (2000).

This paper contained a mistake in Fig. 4a–d. The correct data are described below and are shown on our web site (http://www.med.upenn.edu/~cellbio/arrow.html). The main conclusions remain unchanged. In the paper, we used a LacZ enhancer trap inserted at *Distal-less* to investigate its regulation by *arrow*. However, as both *Distal-less* and *arrow* are on chromosome 2R, the LacZ reporter was flipped away in making *arrow* mutant clones. We have repeated these experiments using anti-Distal-less antibodies generating marked, *Minute+ arrow*^{2} mutant clones. Early-induced *arrow* mutant clones do not survive well; those that do survive exhibit loss of Distal-less expression. Later-induced clones show reduced Distal-less, although there is still residual expression. It is possible that the residual expression is due to perdurance of Arrow protein in cells only recently made mutant for *arrow*. As we stated in the paper, these results with *arrow* are quite similar to those obtained for clones mutant for *frizzled frizzled2* (C. M. Chen and G. Struhl, *Development* **126,** 5441–5452; 1999). In the legend to Fig. 4, however, we noted the higher level of Distal-less expression in the wild-type twin spots compared to the heterozygous tissue. Rather than reflecting changes in Wnt signalling, this resulted simply from the presence of two copies of the Distal-less LacZ reporter on the wild-type twin spots. □

erratum

Polo-like kinase 1 phosphorylates cyclin B1 and targets it to the nucleus during prophase

Fumiko Toyoshima-Morimoti, Eri Taniguchi, Nobuko Shinya, Akihiro Iwamatsu & Eisuke Nishida

Nature **410,** 215–220 (2001).

Figure 5g was printed in black and white instead of in colour. The Figure is reproduced in colour below. □